



# Evaluation of a new dielectric barrier discharge excitation source for the determination of arsenic with atomic emission spectrometry



Zhenli Zhu <sup>a,\*</sup>, Haiyang He <sup>a,b</sup>, Dong He <sup>a,b</sup>, Hongtao Zheng <sup>a,b</sup>, Caixiang Zhang <sup>a</sup>, Shenghong Hu <sup>a,c</sup>

<sup>a</sup> State Key Laboratory of Biogeology and Environmental Geology, China University of Geosciences, Wuhan 430074, China

<sup>b</sup> Faculty of Material Science and Chemistry, China University of Geosciences, Wuhan 430074, China

<sup>c</sup> Faculty of Earth Sciences, China University of Geosciences, Wuhan 430074, China

## ARTICLE INFO

### Article history:

Received 10 December 2013

Received in revised form

21 January 2014

Accepted 24 January 2014

Available online 31 January 2014

### Keywords:

Arsenic

Dielectric barrier discharge

Optical emission spectrometry

Hydride generation

## ABSTRACT

A low power dielectric barrier discharge excitation source was developed to determine arsenic in a cost-effective manner. Arsenic in water was reduced to AsH<sub>3</sub> by hydride generation (HG), which was transported to the miniature dielectric barrier discharge (DBD) excitation source for excitation and optical detection at As 193.7 nm atomic line. The DBD source consists of a quartz tube, a tungsten rod electrode, and a copper coil electrode. The main operation parameters and the potential interferences affecting the determination were investigated. The detection limit for arsenic with the proposed DBD-AES was 4.8 μg L<sup>-1</sup> when the HG products were dried with concentrated H<sub>2</sub>SO<sub>4</sub> before introducing to DBD. Repeatability, expressed as the relative standard deviation of the spectral peak height, was 2.8% (n=11) for 0.1 mg L<sup>-1</sup> arsenic solution. The proposed method was successfully applied to the determinations of certified reference material (GBW08605) and nature water samples.

© 2014 Elsevier B.V. All rights reserved.

## 1. Introduction

Arsenic contamination of groundwater has become a problem of global concern, affecting many developing countries [1]. Current acceptable limit for arsenic in drinking water is 10 μg L<sup>-1</sup> as recommended by the World Health Organization (WHO). Several studies [2–4] pointed out that current commercial available field kits which based on Gutzeit method were not completely reliable for arsenic in groundwater at levels close to the critical regulatory arsenic concentrations of 10 μg L<sup>-1</sup> (the WHO guideline) or the higher Bangladesh standard. Although an arsenic testing campaign to distinguishing safe from unsafe wells was completed in 2004 in Bangladesh, but it cannot completely exclude the dangerous well as the arsenic concentration in a well could change over time [5]. Thus, it is very important to develop a sensitive, reliable and inexpensive unit that could monitor the level of arsenic in water on-site.

In general, the effectiveness and reliability of field test kits are adjudged by comparing their results with those from atomic spectrometry techniques under laboratory conditions [6]. These laboratory-based reference methods, including atomic absorption

spectrometry (AAS), atomic fluorescence spectrometry (AFS) and inductively coupled plasma optical emission spectrometry (ICP-OES)/mass spectrometry (ICP-MS), provide effective approach in determining arsenic with high sensitivity and accuracy [7]. However, conventional atomic spectrometry techniques are unsuitable for field applications because the relevant instruments are bulky, expensive and require high maintenance costs. Therefore, it is highly required to develop miniaturized atomic spectrometer for in-field analysis. In fact, the key issue to develop a portable-atomic spectrometer is the atomizer or emission source [8]. Recently, micro-plasmas have attracted extensive attentions in analytical atomic spectrometry due to their portability and cost-effectiveness [9]. In particular, development of novel emission sources based on micro-plasmas in optical emission spectrometry is the focus of current research. To date, several designs and implementations of micro-plasma emission sources have been reported, including low-power inductively coupled plasma [10,11], low power capacitively coupled plasma [12,13], the low power microwave-induced plasma [14,15], glow discharge [16], electrolyte cathode glow discharge (ELCAD) [17], and dielectric barrier discharge [18–23]. Compared with conventional plasma sources, these micro-plasma sources can miniaturize the entire system and require less power and less gas consumption. Among these instruments, miniature DBD-OES system is one of the most attractive approaches to develop portable-OES due to its unique advantages [20,22,23].

\* Corresponding author. Tel.: +862 767 883 455; fax: +862 767 883 456.

E-mail addresses: [zhuzl03@gmail.com](mailto:zhuzl03@gmail.com), [zizhu@cug.edu.cn](mailto:zizhu@cug.edu.cn) (Z. Zhu).

DBD is a typical technique to generate non-thermal plasma at atmospheric pressure. The DBD plasma is generally operated at slightly above or close to room temperature [24], which is very preferable to compact the instrument equipped with DBD atomizer/emission source for miniaturization. Additionally, DBD generates a large number of high-energy electrons (1–10 eV) at low working temperature, so it shows distinguished capability for dissociation and excitation of analytes [8]. Besides, DBD emission source offers the advantages of small size, low power and low gas consumption, less maintenance costs. All of these advantages indicate that, DBD has the potential to realize the miniaturization of atomic spectrometer. Recently, several investigations based on DBD excitation source have been carried out for the determination of inorganic mercury [19,21,23], thimerosal [25], ammonia [20], nitrogen [26], halohydrocarbons [27], and iodine most recently [22]. Some groups have also developed the methods of As analysis by DBD-AFS [28,29]. However, arsenic determination by DBD-OES has not been established. As well known, hydride generation (HG) coupled to atomic spectrometry has become the mostly used techniques for the determination of elements such as As, Se, Bi, Ge, Sb, Sn and Te due to its high transport efficiency, effective matrix separation and simple operation [30–32]. Unfortunately, HG coupled to the DBD-OES system is very challenging because the excess of co-generated  $H_2$  in HG process may lead to low-power DBD plasma instabilities.

The present work aimed at developing miniature DBD emission source coupled to hydride generation for arsenic determination by optical emission spectrometry. In this study, arsenic in water was reduced to  $AsH_3$  by sodium borohydride and then generated  $AsH_3$  was transported to the miniature DBD emission source for excitation. The parameters affecting arsenic vapor generation in HG process and excitation in DBD were investigated. The analytical performance of HG-DBD-OES system was evaluated. The proposed method was also successfully applied to measure arsenic in certified reference materials and real water samples.

## 2. Experimental

### 2.1. Instrumentation

The HG-DBD-OES system included a hydride generation unit for sample introduction and a DBD optical emission system for As excitation. For HG unit, flow injection operation was performed via

a sequential injection system (Beijing Titan Instruments Co., Ltd., Beijing, China) with two peristaltic pumps and a 6 port selection valve incorporating a 500  $\mu$ L sample loop. The HCl and potassium borohydride solution were pumped by the peristaltic pumps and were mixed in a T-piece where the reaction started. The HG process was accomplished in a polytetrafluoroethylene (PTFE) reaction coil and then the resulted reaction mixture merged with carrier gas (Ar). Separation of volatile  $AsH_3$  was performed in a homemade gas–liquid separator (GLS).

The gaseous  $AsH_3$  was introduced into DBD source for arsenic excitation. As the core unit of the entire system, the homemade cylindrical DBD emission source mainly consisted of a quartz tube, a tungsten rod electrode and a copper coil electrode. The 60 mm long quartz tube (3 mm inner diameter, 5 mm outer diameter) was mounted on a PTFE base. A grounded copper coil was wrapped tightly outside the quartz tube, 10 mm away from the top of the tube. A tungsten rod (1 mm diameter) was centered at the axis of quartz tube as the other electrode. The distance between the tip of the tungsten electrode and the grounded electrode was about 5 mm. When an ac high voltage was applied to the electrodes, discharge plasma was self-ignited upon the tip of the tungsten rod, even appeared outside the quartz tube. The ac high voltage was provided by a CTP-2000 K discharge power supply (Suman Electronics Co., Ltd., Nanjing, China). The input voltage for the discharge power supply was controlled by a TDGC2-1 voltage regulator (CHINT Electric Co., Ltd., China). The discharge gas and sample vapor flowed into the quartz tube through the sample introduction port at the bottom.  $AsH_3$  originating from hydride generation was dissociated and excited in the plasma. The emission signal was measured along the axial direction through the center of the quartz tube. The discharge was imaged 2.5: 1 with a fused-silica lens (focal length=100 mm) to the entrance slit of a monochromator (Princeton Instruments, Action SP2500, focal length=0.5 m) with a 1200 grooves/mm holographic grating. The monochromator is supplied with motorized slits with 3.5 cm height, whose width could be adjusted from 10  $\mu$ m to 3 mm. A Hamamatsu R928 photomultiplier tube was used as the detector.

The schematic diagram of the experimental setup was presented in Fig. 1 and the optimized operating parameters were given in Table 1. An oscilloscope (TDS1000B-SC Tektronix USA) was used to measure the output of the discharge power. The results showed that the output was a 1000 times (with  $\pm 5\%$  vibration) magnified sine wave and frequency was 9.5 kHz. Hydride generation atomic fluorescence spectrometry (AFS-9700,

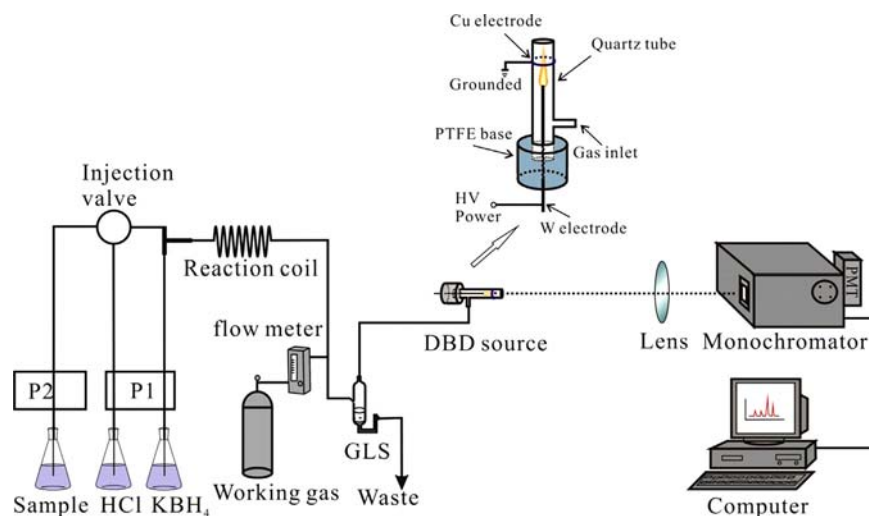


Fig. 1. The schematic diagram of the experimental setup.

**Table 1**  
The optimized instrumental parameters of HG-DBD-OES and HG-AFS.

HG-DBD-OES parameters		HG-AFS parameters	
Negative high voltage of PMT (V)	800	Negative high voltage (V)	780
Integration time of PMT (ms)	100	Lamp primary current (mA)	50
Slit width of Monochromator ( $\mu\text{m}$ )	60	Lamp boost current (mA)	0
Sample loop ( $\mu\text{L}$ )	500	Atomizer observation height(mm)	10
HCl concentration (% v/v)	5	Flow rate of the carrier gas ( $\text{mL min}^{-1}$ )	300
HCl flow rate ( $\text{mL min}^{-1}$ )	4	Flow rate of the shield gas ( $\text{mL min}^{-1}$ )	900
$\text{KBH}_4$ concentration (% m/v)	1%	HCl concentration (% v/v)	5
$\text{KBH}_4$ flow rate ( $\text{mL min}^{-1}$ )	1	$\text{KBH}_4$ concentration (% m/v)	1
Working gas and flow rate ( $\text{mL min}^{-1}$ )	Ar for 260		
Input voltage (V)	26		

Beijing Kechuang Haiguang Instrument Co., Ltd., China) was used to determine the real water samples to validate our results. The operating parameters of HG-AFS were also listed in Table 1.

## 2.2. Reagents and samples

All chemicals were analytical or even higher grade. Argon with a purity of 99.999% was used. Ultrapure water ( $18.2 \text{ M}\Omega \text{ cm}$ , resistivity) used for all the experiments was obtained from a water purification system (9000502, Labconco water props, USA). The 1% (m/v)  $\text{KBH}_4$  solution was prepared by dissolving  $\text{KBH}_4$  powder in a 0.5% (m/v) KOH solution. The stock standard solution of arsenic ( $1000 \text{ mg L}^{-1}$ ) was purchased from National Analysis Center for Iron and Steel (Beijing, China). Working standard solutions were prepared by stepwise dilution of the stock solution. 1% (m/v) ascorbic acid and 1% (m/v) thiourea were added into the resulting solutions for pre-reduction. Single-element standard solutions of  $\text{Cr}^{3+}$ ,  $\text{Mn}^{2+}$ ,  $\text{Fe}^{3+}$ ,  $\text{Co}^{2+}$ ,  $\text{Ni}^{2+}$ ,  $\text{Cu}^{2+}$ ,  $\text{Zn}^{2+}$ ,  $\text{Cd}^{2+}$  and  $\text{Pb}^{2+}$  were used to assess the interferences from individual metals present at concentrations of 1 and  $10 \text{ mg L}^{-1}$  in solutions of  $0.2 \text{ mg L}^{-1}$  arsenic. A solution of 5% (v/v) hydrochloric acid prepared from concentrated HCl was used as carrier solution. All of finally working arsenic solutions (including samples and standards) were acidified by HCl to a concentration of 5% (v/v).

## 3. Results and discussion

HG coupled to the DBD-OES system is very challenging in previous studies mainly because the excess of co-generated  $\text{H}_2$  in HG process may lead to low-power DBD plasma instabilities. Therefore, in our preliminary study, we investigated the DBD plasma stability and the background emission spectra when the Ar-DBD plasma coupled to HG blank solution with 1%  $\text{KBH}_4$  (as Fig. 2 shown). Stable plasma could be readily generated, which indicated that  $\text{H}_2$  generated in HG would not affect the stability of plasma in this cylindrical DBD. Similar to a previous study of CVG-DBD [23], the major contributions to plasma background were the molecular emission of OH bands (bandheads at 281 and 306 nm), the  $\text{N}_2$  second positive system (bandheads at 337, 357, and 380 nm), and some of Ar atomic emission lines. When introduced the sample solution with  $1 \text{ mg L}^{-1}$  arsenic by HG into the Ar-DBD plasma, 5 As I emission lines (193.7, 197.2, 200.3, 228.8, 234.9 nm) could be obviously observed. All these results demonstrated that the DBD with the proposed cylindrical geometric structure had a good compatibility with hydride generation and the effective excitation of arsenic could be obtained by the as-proposed HG-DBD method. The atomic line of 193.7 nm was chosen in following experiments to avoid the possible interference from other elements.

### 3.1. Optimization of experimental conditions

In order to find the optimal conditions for measurement, arsenic emission spectrum from the Ar-DBD was collected with different monochromator slit widths in the first set of experiments. Because the  $60 \mu\text{m}$  slit width gave the greatest signal-to-background intensity ratios (SBR), it was chosen in all experiments. Subsequently, several important parameters such as concentration and flow rate of the reductant, type of discharge gas and input voltage were evaluated by a univariate approach. In this part,  $1 \text{ mg L}^{-1}$  arsenic solutions were used.

#### 3.1.1. Effect of reducing agent concentration and flow rate

It is well known that the concentration of  $\text{KBH}_4$  is critical for the analytical performance of HG (i.e., the generation efficiency of  $\text{AsH}_3$  in this case). In addition, it also affects the DBD micro-plasma due to the amount of  $\text{H}_2$  co-generated. It has been ascertained that the optimal concentration of the reducing agent ranged extensively from 0.25% (m/v) to 10% (m/v), and the 1% (m/v) of  $\text{NaBH}_4$  was the most used [32]. Consistent with the previous results, the maximum of both the net intensity of arsenic and the SBR was obtained with 1% (m/v)  $\text{KBH}_4$  in this work. It should be noted that the intensity and the SBR of As line decreased with increasing  $\text{KBH}_4$  concentration, when it is above 1% (m/v). When the concentration increased to 5% (m/v), the DBD plasma becomes unstable and no arsenic line could be observed. The  $\text{KBH}_4$  flow rate was tested from 0.5 to  $2.5 \text{ mL min}^{-1}$ . The signal intensity significantly decreased when the flow rate beyond  $1.0 \text{ mL min}^{-1}$ . It may be explained by that the generated  $\text{H}_2$  diluted the As species and decreased the intensity of DBD plasma. Thus, 1% (m/v)  $\text{KBH}_4$  solution was selected and the optimal flow rate was set as  $1 \text{ mL min}^{-1}$ .

#### 3.1.2. Effect of working gas

In this system, the working gas not only acts as carrier gas to bring the  $\text{AsH}_3$  into the DBD plasma, but also supports the discharge. Two different kinds of gas, argon and helium, were studied. Although the plasmas were generated easily both in argon and in helium, the background spectra of plasmas were very different. It was observed that the emission intensity of He-DBD was far below the intensity of Ar-DBD when their flow rates are the same. More importantly, it was difficult to distinguish arsenic emission signal in HG-He-DBD. Thus argon is chosen to determine arsenic. The maximum signal of arsenic was obtained at the flow rate of  $260 \text{ mL min}^{-1}$  with Ar. This may be explained by that, low flow rate may result in inefficient separation and transport of analyte from the GLS to DBD and high flow rate could dilute the sample and reduce the residence time in the discharge plasma. Therefore,  $260 \text{ mL min}^{-1}$  of Ar was employed in subsequent experiments.

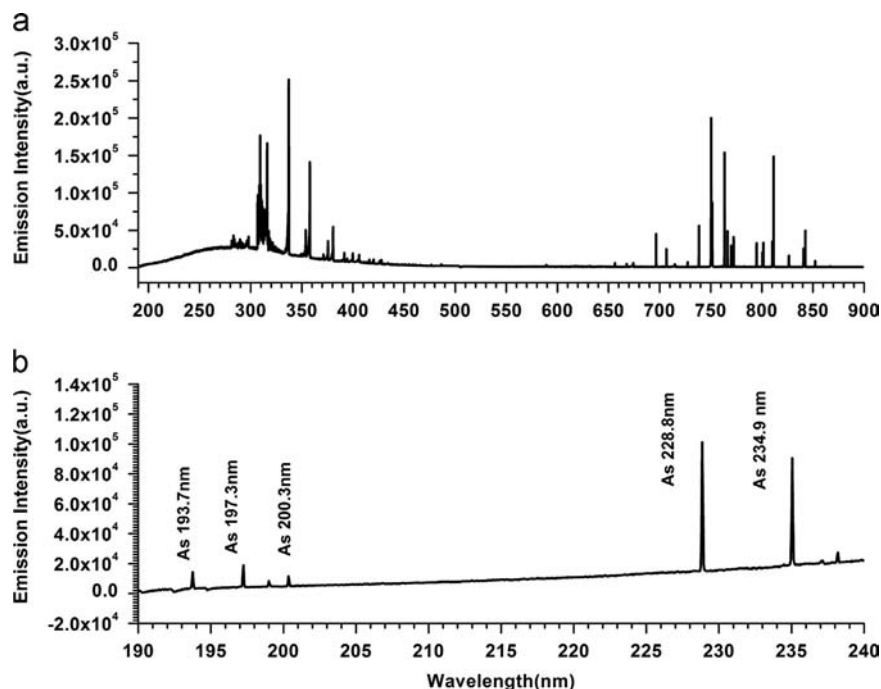


Fig. 2. Typical HG-Ar-DBD emission spectra of (a) an acid blank solution (HCl, 5%) and (b) that spiked with As at  $1 \text{ mg L}^{-1}$ .

### 3.1.3. Effect of HCl solution flow rate

HCl solution with concentration of 5% (v/v) was employed as carrying solution in this flow injection HG system. The influence of HCl solution flow rate was studied in the range of  $1\text{--}5 \text{ mL min}^{-1}$ . The results showed that, the peak area of the arsenic signal was almost identical when the flow rate increased from 1 to  $4 \text{ mL min}^{-1}$ . In contrast, the net peak height increased with flow rate in this range, and the maximum peak height intensity was found at  $4 \text{ mL min}^{-1}$ . Flow rate higher than  $4 \text{ mL min}^{-1}$  decreases both peak height and peak area signal responses, which may be caused by reduced reaction time of the sample in HG reactor. Therefore, HCl solution flow rate of  $4 \text{ mL min}^{-1}$  was selected in following experiments.

### 3.1.4. Effect of input voltage

The influence of the input voltage on the response of emission intensity was shown in Fig. 3. An Ar-DBD was quickly generated as soon as power is applied to the electrodes with an input voltage ranging from 22 V to 26 V in which range the DBD-plasma can keep stable. A voltage regular was used to control the input voltage. Both net peak height and SBR of response signals of As increased when the input voltage rose from 22 V to 26 V (as shown in Fig. 3). Thus, 26 V was employed as the optimum input voltage in subsequent studies. It was worthy to note that the total input power of DBD is less than 30 W, which indicates the possibility of operating the DBD source with a battery-powered supply.

## 3.2. Interference

The interferences caused by a series of metal elements including  $\text{Cr}^{3+}$ ,  $\text{Mn}^{2+}$ ,  $\text{Fe}^{3+}$ ,  $\text{Co}^{2+}$ ,  $\text{Ni}^{2+}$ ,  $\text{Cu}^{2+}$ ,  $\text{Zn}^{2+}$ ,  $\text{Cd}^{2+}$  and  $\text{Pb}^{2+}$  in determining  $0.2 \text{ mg L}^{-1}$  arsenic using FI-HG-DBD-OES method were examined and the results were summarized in Table 2. All interferences were tested at concentration of  $1 \text{ mg L}^{-1}$  and  $10 \text{ mg L}^{-1}$ . The recoveries were all in the range of 94.2–107.8%, which implied our proposed method was free of interference from those coexisting ions in the studied concentration range. These results demonstrated that the HG-DBD-OES provided a robust method for As determination.

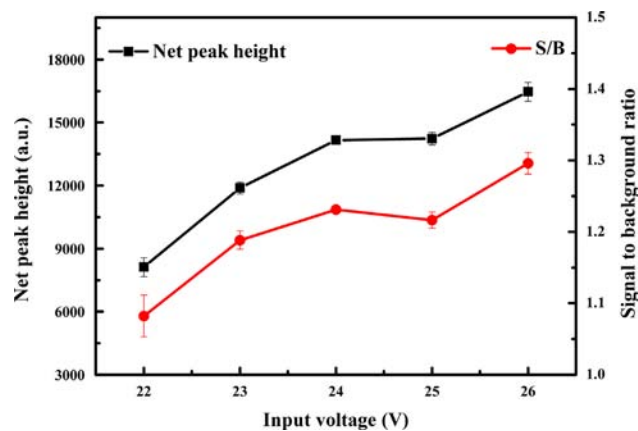


Fig. 3. Optimization of the input voltage ( $n=3$ ).

Table 2

Interferences from metal elements (as concentration:  $0.2 \text{ mg L}^{-1}$ ,  $n=4$ ).

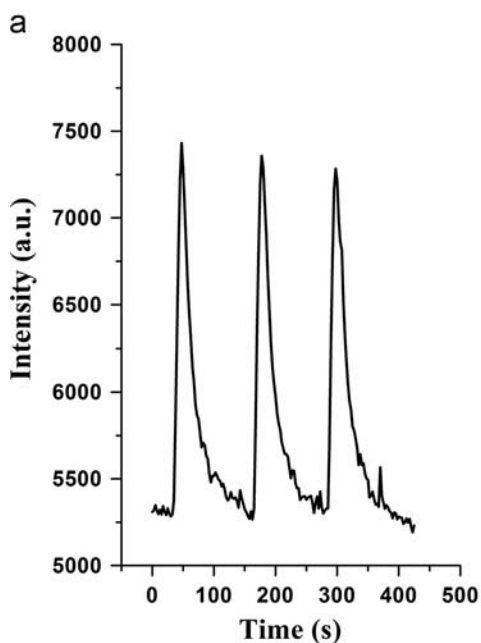
Element	Concentration ( $\text{mg L}^{-1}$ )	Recovery (%)	Element	Concentration ( $\text{mg L}^{-1}$ )	Recovery (%)
$\text{Cr}^{3+}$	1	$100.3 \pm 1.2$	$\text{Cr}^{3+}$	10	$102.9 \pm 3.4$
$\text{Mn}^{2+}$	1	$104.0 \pm 0.9$	$\text{Mn}^{2+}$	10	$98.5 \pm 1.2$
$\text{Fe}^{3+}$	1	$94.2 \pm 2.9$	$\text{Fe}^{3+}$	10	$103.3 \pm 3.9$
$\text{Co}^{2+}$	1	$97.3 \pm 2.5$	$\text{Co}^{2+}$	10	$98.8 \pm 2.4$
$\text{Ni}^{2+}$	1	$101.0 \pm 1.1$	$\text{Ni}^{2+}$	10	$101.1 \pm 1.5$
$\text{Cu}^{2+}$	1	$97.2 \pm 5.4$	$\text{Cu}^{2+}$	10	$100.2 \pm 1.5$
$\text{Zn}^{2+}$	1	$101.2 \pm 4.3$	$\text{Zn}^{2+}$	10	$99.2 \pm 0.6$
$\text{Cd}^{2+}$	1	$96.5 \pm 2.5$	$\text{Cd}^{2+}$	10	$100.9 \pm 1.5$
$\text{Pb}^{2+}$	1	$107.8 \pm 5.4$	$\text{Pb}^{2+}$	10	$99.1 \pm 3.2$

## 3.3. Analytical performance and figures of merit

The analytical performance of HG-DBD-OES was evaluated under optimal operating conditions. With the emission spectral peak height at the 193.7 nm as a quantitative parameter, the

calibration curve built with data from standard arsenic solutions with concentration ranging from 50 to 500  $\mu\text{g L}^{-1}$  provided linear correlation coefficients ( $R$ ) better than 0.99. The limit of detection (LOD) was calculated using the definition  $3\sigma/m$  ( $\sigma$  is the standard deviation of 11 measurements of the blank and  $m$  is the slope of the calibration curve). The LOD for arsenic was calculated to be 22.3  $\mu\text{g L}^{-1}$ .

We found that the introduction of water vapor into the DBD plasma significantly reduce the emission intensity, which was similar to our previous study [23]. Therefore, the effect of the residual water vapor on the arsenic emission signal was also investigated and shown in Fig. 4. The moisture from the vapor was removed by passing the HG-generated gaseous products, collected at the exit of the GLS, through a vessel containing concentrated  $\text{H}_2\text{SO}_4$  before its introduction into the DBD plasma. The arsenic emission intensity became much stronger when the water vapor was removed. Although the background emission intensity also increased, better SBR could be obtained with moisture removal. Based on these results, the analytical performance of the FI-HG-DBD-OES method with removal of residual moisture was also investigated and summarized in Table 3. The LOD for arsenic was 4.6-fold lower in the case of removing water vapor. Subsequently the repeatability on FI-HG-DBD-OES method with removing moisture was studied. The relative standard deviation of the spectral peak height was 2.8% ( $n=11$ ) for 0.1  $\text{mg L}^{-1}$  arsenic standard solution. All these results indicated that our proposed DBD-OES has good sensitivity and repeatability and it could be used for the direct measurement of As in water samples (Fig. 5).



### 3.4. Analytical application

The proposed method was applied to the determination of arsenic in real water samples. One certified reference materials of water (GBW08605) were chosen to verify the accuracy of the system. Subsequently, some real water samples were determined by the as-proposed FI-HG-DBD-OES method and the results were

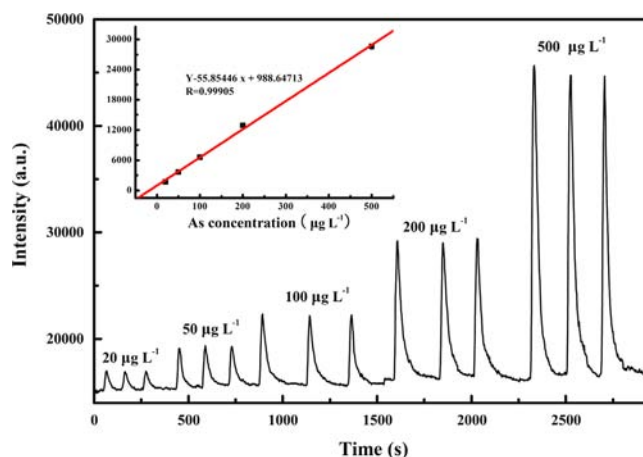


Fig. 5. Calibration curve and temporal profiles of the Ar-DBD coupled with flow injection with the removal of residue moisture. Peaks were obtained with standard solutions having As concentrations between 20 and 500  $\mu\text{g L}^{-1}$ . The inset shows the calibration curve with peak height as the analytical parameter.

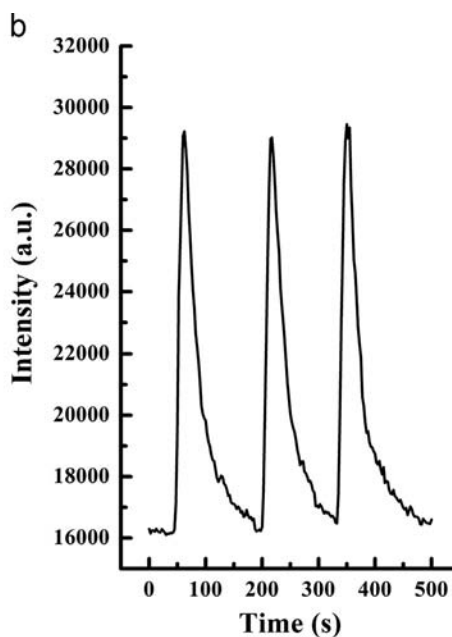


Fig. 4. Effect of residual water vapor on arsenic emission from the Ar-DBD. (a) without removal of residual moisture; (b) with removal of residual moisture.

**Table 3**  
The calibration curves and LODs for arsenic by FI-HG-DBD-OES method.

Method	Linear range ( $\mu\text{g L}^{-1}$ )	Regression equation <sup>a</sup>	$R$	LOD ( $\mu\text{g L}^{-1}$ )
Without removal of residual moisture	50–500	$I = 8.067C + 309.8$	0.998	22.3
With removal of residual moisture	20–500	$I = 55.85C + 988.6$	0.999	4.8

<sup>a</sup> I: The intensity of peak height; C: The concentration of arsenic

**Table 4**

The analytical performance of the proposed HG-DBD-OES compared with other studies of As.

Reference	LOD	RSD and detect concentration
This study	4.8 $\mu\text{g L}^{-1}$	2.8% ( $n=11$ ), 100 $\mu\text{g L}^{-1}$
USN/UV-MIP-OES <sup>a</sup> [33]	11 $\mu\text{g L}^{-1}$	3% ( $n=5$ ), 550 $\mu\text{g L}^{-1}$
$\mu\text{chip-CE-HG-MIP-OES}$ <sup>b</sup> [34]	3.9 $\mu\text{g L}^{-1}$ (As)	5% ( $n=6$ ), 50 $\mu\text{g L}^{-1}$
	5.4 $\mu\text{g L}^{-1}$ (As V)	7% ( $n=6$ ), 50 $\mu\text{g L}^{-1}$
HG-ICP-OES [35]	121 $\mu\text{g L}^{-1}$	0.6% ( $n=3$ ), 200 $\mu\text{g L}^{-1}$
HG-ICP-OES [36]	30 $\mu\text{g kg}^{-1}$	0.2% ( $n=10$ ), 200 $\mu\text{g L}^{-1}$

<sup>a</sup> Ultrasonic nebulization/ultraviolet photolysis interfaced with microwave induced plasma optical emission spectrometry.

<sup>b</sup> Microfluidic chip-based capillary electrophoresis interfaced with microwave induced plasma optical emission spectrometry.

**Table 5**

Analytical results of for the determination of arsenic ( $n=3$ ) in water samples by FI-HG-DBD-OES and by HG-AFS.

Sample <sup>a</sup>	Found by DBD-AES ( $\mu\text{g L}^{-1}$ )	Certified value or found by HG-AFS ( $\mu\text{g L}^{-1}$ )
GBW08605	510.4 $\pm$ 11.9	500.0 $\pm$ 7.5 (certified value)
1 <sup>b</sup>	115.7 $\pm$ 10.8	125.5 $\pm$ 1.0 (HG-AFS)
2 <sup>c</sup>	197.5 $\pm$ 5.1	180.0 $\pm$ 3.5 (HG-AFS)
3 <sup>d</sup>	448.9 $\pm$ 11.6	481.3 $\pm$ 6.5 (HG-AFS)

<sup>a</sup> Sampling point.

<sup>b</sup> 39°36.413 N; 113°09.299 E.

<sup>c</sup> 39°30.502 N; 113°00.611 E.

<sup>d</sup> 39°25.230 N; 112°56.758 E.

compared with conventional HG-AFS. As indicated by Table 4, all results obtained with HG-DBD-OES were in good agreement with certified values or values from HG-AFS Table 5.

#### 4. Conclusions

We developed a sensitive, simple and miniature DBD emission source for determination of arsenic in natural water samples. The proposed cylindrical DBD plasma could be readily coupled to hydride generation and the plasma source could excite arsenic effectively. It offers several important advantages over other emission sources: low power consumption (< 30 W), low gas consumption ( $\leq$  260 mL  $\text{min}^{-1}$ ), small size, and ease of fabrication. The HG-DBD-OES system can be applied for arsenic determination in water samples with satisfying reliability and repeatability. With all these merits, integration of the proposed cylindrical DBD source with a portable optical emission spectrometer provides with potential for developing inexpensive, robust and portable optical emission device for in-field arsenic determination. Moreover, HG-DBD-OES system can be used to determine other hydride-forming elements (e.g. Se, Sb, Cd, etc) simultaneously.

#### Acknowledgments

We gratefully acknowledge the financial support from the National Nature Science Foundation of China (No. 21375120 and No. 41173018), the R&D Special Fund for Public Welfare Industry of Hubei province (2012DCA19001), and the Fundamental Research Funds for the Central Universities (CUG120117, CUG120502), China University of Geosciences (Wuhan).

#### References

- [1] A. Mukherjee, M.K. Sengupta, M.A. Hossain, S. Ahamed, B. Das, B. Nayak, D. Lodh, M.M. Rahman, D. Chakraborti, J. Health Popul. Nutr. 24 (2006) 142–163.
- [2] M.M. Rahman, D. Mukherjee, M.K. Sengupta, U.K. Chowdhury, D. Lodh, C.R. Chanda, S. Roy, M. Selim, Q. Quamruzzaman, A.H. Milton, S. M. Shahidullah, M.T. Rahman, D. Chakraborti, Environ. Sci. Technol. 36 (2002) 5385–5394.
- [3] B.E. Erickson, Environ. Sci. Technol. 37 (2003) 35A–38A.
- [4] N.R. Khandaker, Environ. Sci. Technol. 38 (2004) 479A–479A.
- [5] J.G. Thundiyil, Y. Yuan, A.H. Smith, C. Steinmaus, Environ. Res. 104 (2007) 367–373.
- [6] J. Feldmann, in: H. Garelick, H. Jones (Eds.) Reviews of Environmental Contamination and Toxicology, vol. 197: Arsenic Pollution and Remediation: An International Perspective, 2008, pp. 61–75.
- [7] P. Grinberg, R.E. Sturgeon, J. Anal. At. Spectrom. 24 (2009) 508–514.
- [8] J. Hu, W. Li, C. Zheng, X. Hou, Appl. Spectrosc. Rev. 46 (2011) 368–387.
- [9] V. Karanassios, Spectrochim. Acta B 59 (2004) 909–928.
- [10] O.B. Minayeva, J.A. Hopwood, J. Anal. At. Spectrom. 17 (2002) 1103–1107.
- [11] O.B. Minayeva, J.A. Hopwood, J. Anal. At. Spectrom. 18 (2003) 856.
- [12] T. Frentiu, A.I. Mihaltan, M. Ponta, E. Darvasi, M. Frentiu, E. Cordos, J. Hazard. Mater. 193 (2011) 65–69.
- [13] T. Frentiu, D. Petreus, M. Senila, A.I. Mihaltan, E. Darvasi, M. Ponta, E. Plaian, E.A. Cordos, Microchem. J. 97 (2011) 188–195.
- [14] P. Pohl, I. Jimenez Zapata, E. Voges, N.H. Bings, J.A.C. Broekaert, Microchim. Acta 161 (2007) 175–184.
- [15] P. Pohl, I.J. Zapata, N.H. Bings, E. Voges, J.A.C. Broekaert, Spectrochim. Acta B 62 (2007) 444–453.
- [16] J.C.T. Eijkel, H. Stoeri, A. Manz, J. Anal. At. Spectrom. 15 (2000) 297–300.
- [17] T. Cserfalvi, P. Mezei, J. Anal. At. Spectrom. 9 (1994) 345.
- [18] W.S. Abdul-Majeed, J.H. Parada, W.B. Zimmerman, Anal. Bioanal. Chem. 401 (2011) 2713–2722.
- [19] M. Puanngam, S. Ohira, F. Unob, J.H. Wang, P.K. Dasgupta, Talanta 81 (2010) 1109–1115.
- [20] Z. Wu, M. Chen, P. Li, Q. Zhu, J. Wang, Analyst 136 (2011) 2552–2557.
- [21] Y. Yu, Z. Du, M. Chen, J. Wang, Angew. Chem. Int. Ed. 47 (2008) 7909–7912.
- [22] Y.L. Yu, S. Dou, M.L. Chen, J.H. Wang, Analyst 138 (2013) 1719–1725.
- [23] Z. Zhu, G.C. Chan, S.J. Ray, X. Zhang, G.M. Hieftje, Anal. Chem. 80 (2008) 8622–8627.
- [24] O. Motret, C. Hibert, S. Pellerin, J.M. Pouvesle, J. Phys. D-Appl. Phys. 33 (2000) 1493–1498.
- [25] H. He, Z. Zhu, H. Zheng, Q. Xiao, L. Jin, S. Hu, Microchem. J. 104 (2012) 7–11.
- [26] W. Li, X. Jiang, K. Xu, X. Hou, C. Zheng, Microchem. J. 99 (2011) 114–117.
- [27] W. Li, C. Zheng, G. Fan, L. Tang, K. Xu, Y. Lv, X. Hou, Anal. Chem. 83 (2011) 5050–5055.
- [28] Y.-L. Yu, Z. Du, M.-L. Chen, J.-H. Wang, J. Anal. At. Spectrom. 23 (2008) 493–499.
- [29] Z. Zhu, J. Liu, S. Zhang, X. Na, X. Zhang, Anal. Chim. Acta 607 (2008) 136–141.
- [30] Z. Benzo, M.N. Matos-Reyes, M.L. Cervera, M. de la Guardia, J. Braz. Chem. Soc. 22 (2011) 1782–1787.
- [31] P. Pohl, R.E. Sturgeon, Trac-Trends Anal. Chem. 29 (2010) 1376–1389.
- [32] P. Pohl, Trac-Trends Anal. Chem. 23 (2004) 87–101.
- [33] H. Matusiewicz, M. Slachcinski, Spectr. Lett. 46 (2013) 315–326.
- [34] H. Matusiewicz, M. Slachcinski, Microchem. J. 102 (2012) 61–67.
- [35] A. Ilander, A. Vaisanen, Anal. Chim. Acta. 689 (2011) 178–183.
- [36] W.d.L. Lopes, R.E. Santelli, E.P. Oliveira, M.d.F. Batista de Carvalho, M.A. Bezerra, Talanta 79 (2009) 1276–1282.